Hindawi Publishing Corporation
Mathematical Problems in Engineering
Volume 2012, Article ID 298413, 11 pages
doi:10.1155/2012/298413

Research Article

The Response Frequency Conversion Characteristic of a Nonlinear Curved Panel with a Centre Mass and the Sound Radiations

Y. Y. Lee

Department of Civil and Architectural Engineering, City University of Hong Kong, Kowloon Tong, Kowloon, Hong Kong

Correspondence should be addressed to Y. Y. Lee, bcraylee@cityu.edu.hk

Received 4 July 2012; Accepted 30 August 2012

Academic Editor: Xing-Gang Yan

Copyright © 2012 Y. Y. Lee. This is an open access article distributed under the Creative Commons Attribution License, which permits unrestricted use, distribution, and reproduction in any medium, provided the original work is properly cited.

This study investigates the response frequency conversion characteristic of a nonlinear curved panel mounted with a centre mass and the sound radiations. A set of coupled governing differential equations is set up and used to generate the nonlinear vibration responses, which are used to calculate the corresponding radiated sounds. The vibration, sound levels, and the ratio of the antisymmetrical to symmetrical mode responses are plotted against the excitation level and compared with a set of experimental data. The frequency conversion characteristic is investigated from the frequency spectrums of the vibration responses.

1. Introduction

Previous studies of various nonlinear vibration/oscillation systems have been studied over recent decades [1–15]. Some researchers particularly worked on nonlinear curved/buckled beams/plates. Detailed discussions on the quadratic nonlinear responses of a two-degrees-of-freedom beam-mass system can be found in the work of Nayfeh and Mook [16] and Schmidt and Tondl [17]. Besides, some previous studies [18, 19] have shown that the nonlinear antisymmetric mode responses of a curved panel can be excited symmetrically due to the quadratic nonlinearity. It was found that the dominant response frequency was much lower than the excitation frequency. However, there are few research works which focus on the sound radiation of a nonlinear structure. In this study, the response frequency conversion characteristic of nonlinear curved panel vibrations and the sound radiations are further investigated in detail. In order to observe the frequency conversion characteristics, the resonant frequencies of the first symmetrical and antisymmetrical modes of the panel have to be tuned

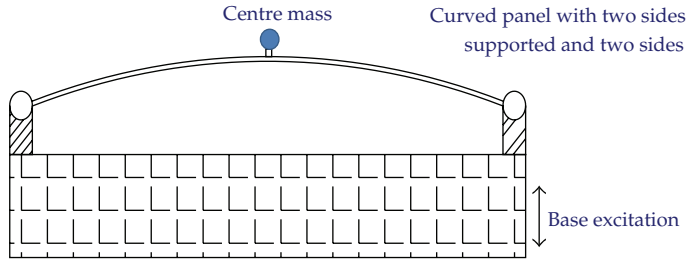

Figure 1: Side view of a curved panel mounted with a mass.

close to each other. According to the experimental experience documented in [20], adding masses on the panel surface makes easier for tuning of the resonant frequencies of a curved panel in a particular range. That is why a centre mass is considered and mounted on the panel in this study.

2. Methodology

Figure 1 shows a simply supported curved panel mounted with a central mass that is subject to a harmonic excitation. It is assumed that the flexural bending along the width is neglected. Thus, the structure is simplified and considered as a beamlike panel. The governing differential equation of a curved structure with a centre mass that is subject to a harmonic uniformly distributed pressure force [19] is given by

$$(\rho A + M)\ddot{w} + \Omega\dot{w} + EIw'''' = \frac{EA}{L}(w'' + \overline{w}'')\int_0^L \left(\overline{w}'w' + \frac{1}{2}(w')^2\right)dx - \kappa(\rho A + M)g\sin(\omega t), \tag{2.1}$$

where w is the transverse displacement caused by the panel bending; $\dot{w}$ and $\ddot{w}$ are the first and second derivatives of the transverse displacement with respect to time t; w', w'', and w'''' are the first, second, and fourth derivatives of the transverse displacement with respect to the spatial variable x; $\overline{w} = q_0\phi_1$ is the initial transverse displacement; q_0 is the transverse displacement at the center; E is the Young's modulus; ρ is the material density; Ω is the damping coefficient; A is $B\times h$ = the cross-sectional area; B is the width; h is the thickness; L is the length; M is $m_c\delta(L/2)$; m_c is the center mass; $\delta(x)$ is the Dirac delta function; ω is the excitation frequency; κ is the excitation parameter; g is gravity is 9.81 ms^{-2}. The transverse displacement is expressed in terms of the mode shapes and given by

$$w(x,t) = \sum_{i=1}^{N} q_i(t)\phi_i(x), \tag{2.2}$$

where q_i is the modal amplitude of the ith mode; ϕ_i is the ith sine function mode shape (i.e. $\sin(i\pi x/L)$); i is the mode number; N is the number of modes considered (only the first three modes are considered in this study). According to [21], the resonant frequency of a nonlinear

isotopic simply supported beam/plate can be accurately obtained using the single-mode approach. Hence, (2.1) can be easily reduced into a Duffing equation which has been solved by various methods (e.g. the variational approach [2], Hamiltonian approach [3, 4], elliptical Integral method [8], the harmonic balance method [8], the numerical integration method [18, 19], etc.). In Appendix, the procedure to obtain the resonant frequency of the Duffing equation is shown.

The residual can be found by substituting (2.2) into (2.1) and then multiplied by ϕ_i, integrated with respect to the beam length, and set it to zero. A set of weighted residual differential equations is generated (see (2.3)-(2.4)). These differential equations can be solved using the Runge-Kutta numerical integration to obtain the modal responses

$$\begin{aligned}\Delta = {} & (\rho A + M)\sum_{i=1}^{N}\ddot{q}_i\phi_i + \xi\omega_i\sum_{i=1}^{N}\dot{q}_i\phi_i + EI\sum_{i=1}^{N}q_i\phi_i'''' - \frac{EA}{L}\left(\sum_{i=1}^{N}q_i\phi_i'' + q_0\phi_1''\right) \\ & \times\left(\sum_{i=1}^{N}q_0q_i\int_0^L\phi_1'\phi_i'dx + \frac{1}{2}\sum_{i=1}^{N}\sum_{j=1}^{N}q_iq_j\int_0^L\phi_i'\phi_j'dx\right) + F,\end{aligned} \tag{2.3}$$

$$\begin{aligned}& \sum_{i=1}^{N}\ddot{q}_i\left(\rho A\alpha_{i,m}^{0,0} + m_c\beta_{i,m}\right) + \sum_{i=1}^{N}\dot{q}_i\xi\omega_i\alpha_{i,m}^{0,0} + EI\sum_{i=1}^{N}q_i\alpha_{i,m}^{4,0} - \frac{EA}{L} \\ & \times\left[+\sum_{i=1}^{N}\alpha_{1,i}^{1,1}\alpha_{1,m}^{2,0}q_0^2q_i + \sum_{i=1}^{N}\sum_{j=1}^{N}\left(\alpha_{1,i}^{1,1}\alpha_{j,m}^{2,0} + \frac{1}{2}\alpha_{i,j}^{1,1}\alpha_{1,m}^{2,0}\right)q_0q_iq_j + \frac{1}{2}\sum_{i=1}^{N}\sum_{j=1}^{N}\sum_{k=1}^{N}\alpha_{i,j}^{1,1}\alpha_{k,m}^{2,0}q_iq_jq_k\right] \\ & + F_m = 0,\end{aligned} \tag{2.4}$$

where ϕ_i', ϕ_i'', and ϕ_i'''' are the first, second, and fourth derivatives of the ith mode shape, respectively, and i, j, m, k are the mode numbers. $\xi\omega_i = \Omega$, where ξ is the modal damping coefficient

$$F = \kappa(\rho A + M)g\sin(\omega t), \tag{2.5a}$$

$$F_m = \int_0^L F\phi_m dx, \qquad \beta_{i,m} = \phi_i\left(\frac{L}{2}\right)\phi_m\left(\frac{L}{2}\right), \tag{2.5b}$$

$$\alpha_{i,m}^{0,0} = \int_0^L\phi_i\phi_m dx, \tag{2.5c}$$

$$\alpha_{i,m}^{2,0} = \int_0^L\phi_i''\phi_m dx, \tag{2.5d}$$

$$\alpha_{i,m}^{4,0} = \int_0^L\phi_i''''\phi_m dx. \tag{2.5e}$$

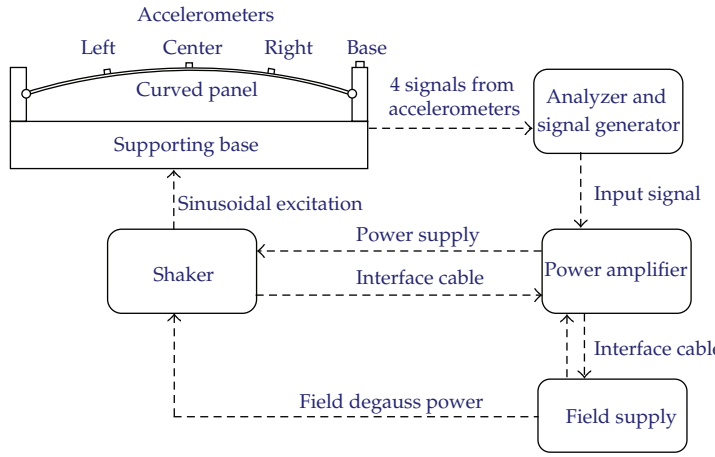

Figure 2: Experimental setup.

Then, the sound power radiated from the ith mode can be calculated using the radiation efficiency formulas which have been adopted in [22, 23]. The following two formulas are the simplified version in [22] for quick calculation:

$$\sigma_i = \frac{32K^2BL}{i^2\pi^5}\left\{1 - \frac{K^2BL}{12}\left[\left(1 - \frac{8}{(i\pi)^2}\right)\frac{L}{B} + \left(1 - \frac{8}{\pi^2}\right)\frac{B}{L}\right]\right\}, \quad \text{for symmetric modes,} \tag{2.6a}$$

$$\sigma_i = \frac{8K^4BL}{3i^2\pi^5}\left\{1 - \frac{K^2BL}{20}\left[\left(1 - \frac{8}{(i\pi)^2}\right)\frac{L}{B} + \left(1 - \frac{24}{\pi^2}\right)\frac{B}{L}\right]\right\}, \quad \text{for antisymmetric modes,} \tag{2.6b}$$

where $K = \omega/C_{\text{air}}$, C_{air} = sound speed in air.

The experimental setup, which was the same as that in [19], contained a curved steel panel with a thickness of 0.5 mm, an arc length of 310 mm, and a breadth of 350 mm (see Figure 2). It was mounted with a centre mass of 20 g. The first symmetrical and antisymmetrical mode resonant frequencies are $\omega_{\text{sym}} = 101$ and $\omega_{\text{anti}} = 50$ Hz, respectively (i.e. $\omega_{\text{sym}}/\omega_{\text{anti}} \approx 2$). Note that the structure was not perfectly simply supported. The curved panel was sinusoidally excited by a shaker table. The modal vibrations of the structure and the base frame were measured using accelerometers placed at $x = L/4$, $L/2$, and $3/4L$, while another accelerometer was used to monitor the dynamic response of the shaker table.

3. Results and Discussions

In Figure 3(a), the relative total vibration levels are plotted against the excitation parameter, κ. The dimensions of the curved panel are the same as those in the experimental setup. The modal damping coefficient is equal to $\xi = 0.02$. The centre mass is also equal to 20 g. The ratios of the resonant frequencies of the first symmetrical and antisymmetrical modes are tuned to

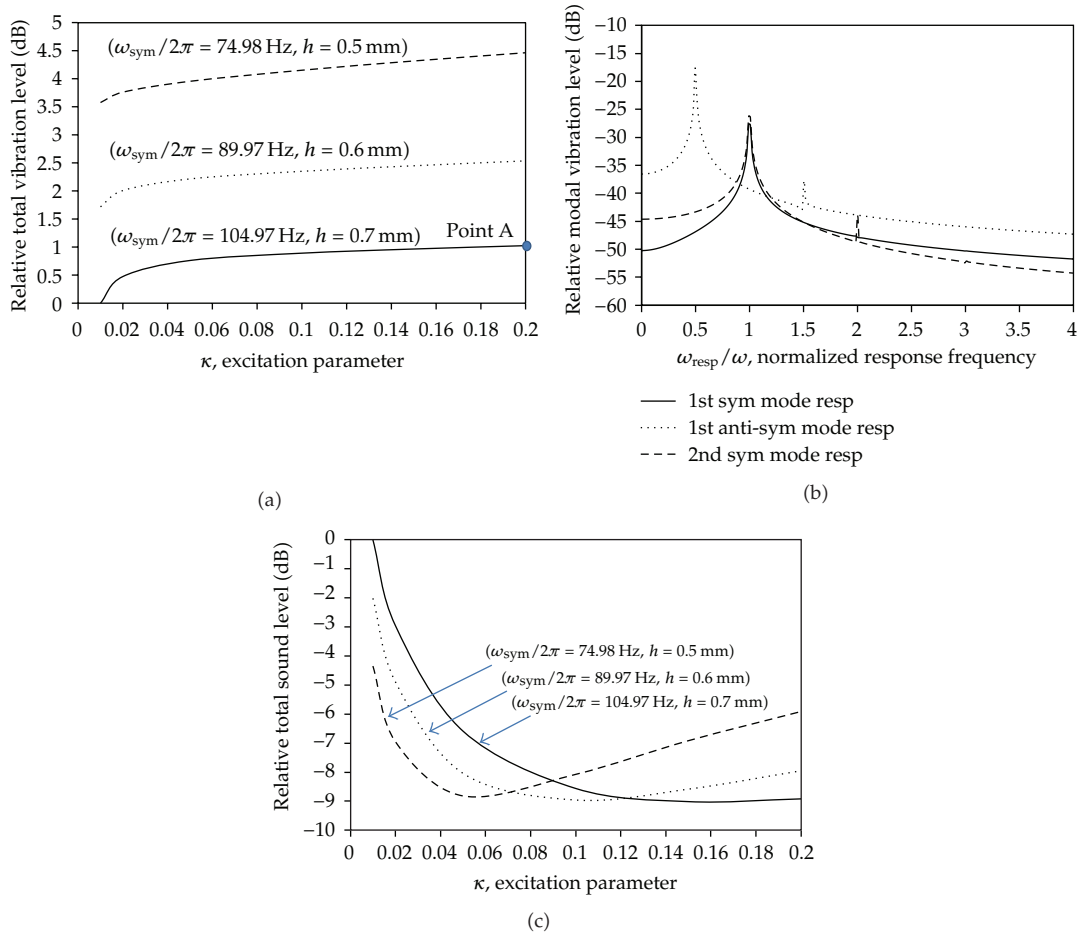

Figure 3: (a) Relative total vibration level ($\omega_{sym}/\omega_{anti\text{-}sym} = 2$, $\omega = \omega_{sym}$), (b) relative modal vibration levels of point A in (a), (c) relative total sound level ($\omega_{sym}/\omega_{anti} = 2$, $\omega = \omega_{sym}$).

two by adjusting the curvature or the initial centre deflection. The vibration level in the case of ($h = 0.7$ mm at $\kappa = 0.01$) is normalized as zero. The total vibration levels are monotonically increasing for all cases. The excitation frequency is equal to the resonant frequency of the first mode. Generally, the thinner the panel is, the higher the vibration level is. Figure 3(b) shows the frequency spectrum of the point A marked in Figure 3(a). It can be seen that the response frequency of the dominant mode, which is the first antisymmetrical mode, is much lower than the excitation frequency (only one-half!). This phenomenon is described as "high-frequency excitation input-low-frequency response output." The response frequencies of the first and second symmetrical modes are the same as the excitation frequency, but the modal vibration amplitudes of the first and second symmetrical modes are much lower than that of the first antisymmetrical mode (even though the excitation and the structure are symmetrical). In Figure 3(c), the relative total radiated sound levels of the three cases are plotted against the normalized excitation. The sound level of the solid line is exponentially deceasing and almost constant for $\kappa > 0.1$. The sound level of the dotted line is exponentially deceasing for $\kappa < 0.1$, bottom around $\kappa = 0.1$, and slowly increasing for $\kappa > 0.1$. Similarly, the sound level of the dash

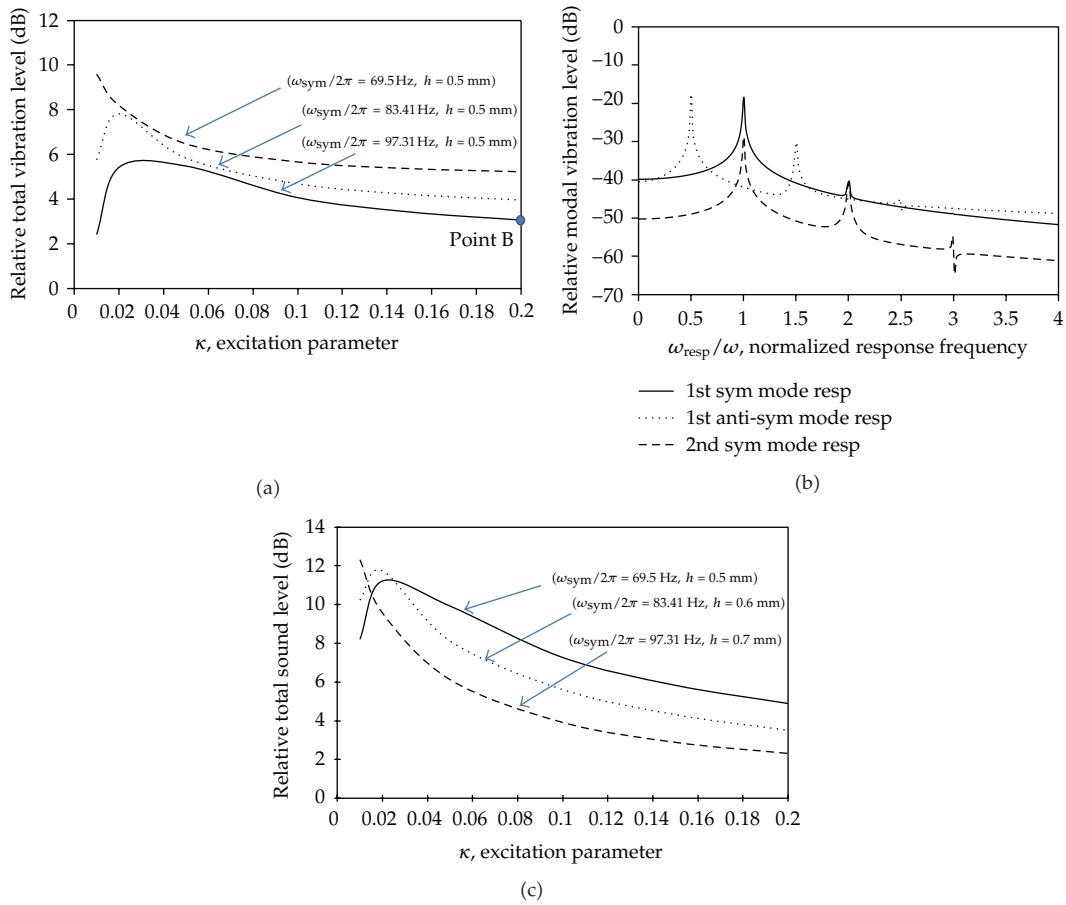

Figure 4: (a) Relative total vibration level ($\omega_{\text{sym}}/\omega_{\text{anti-sym}} = 1.85$, $\omega = \omega_{\text{sym}}$), (b) relative modal vibration levels of point B in (a), (c) relative total sound level ($\omega_{\text{sym}}/\omega_{\text{anti}} = 1.85$, $\omega = \omega_{\text{sym}}$).

line is exponentially deceasing for $\kappa < 0.04$, bottom around $\kappa = 0.04$, and slowly increasing for $\kappa > 0.04$. It is found that although the sound level of the solid line is the highest for $\kappa < 0.1$, the corresponding vibration level is always the lowest; on the contrary, the sound level of the dash line is highest for $\kappa < 0.07$, the corresponding vibration level is always the highest. It is because the radiation efficiency of the first antisymmetric mode is much lower than the others, and thus the overall sound radiation is smaller.

Figure 4(a) shows other 3 cases in which the ratios of the resonant frequencies are not tuned to two. No centre mass is considered in these 3 cases. The vibration level of the thinnest beam is monotonically deceasing. For the other two cases in Figure 4(a), the vibration levels increase from $\kappa = 0.01$ to 0.02, peak around $\kappa = 0.02$ to 0.03, and decease $\kappa = 0.03$ to 0.2. Figure 4(b) shows the frequency spectrum of the point B marked in Figure 4(a). It can be seen that the first antisymmetrical mode is not as dominant as the one in Figure 3(b). It is because the ratio of the resonant frequencies is not tuned to two. The vibration levels of the first symmetrical and antisymmetrical modes are almost equal and much higher than that of the second symmetrical mode. In Figure 4(c), the relative total radiated sound levels of the three

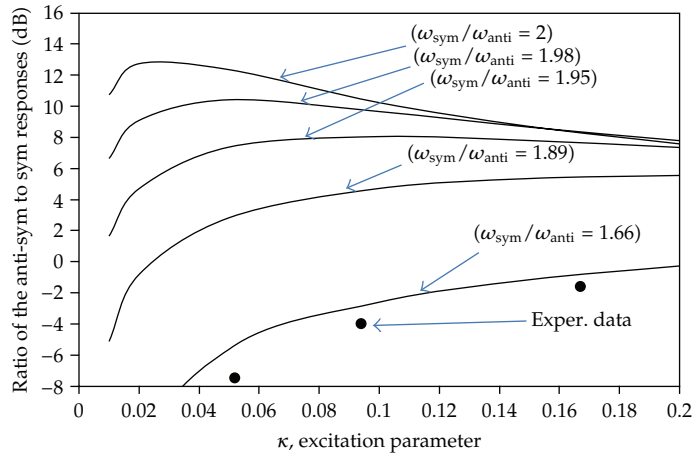

Figure 5: Ratio of the antisymmetrical to symmetrical responses, (dB scale).

cases in Figure 4(a) are plotted against the normalized excitation. The sound level of the dash line is exponentially deceasing. The sound levels of the solid and dotted lines are increasing for $\kappa < 0.03$, peak around $\kappa = 0.03$, and decreasing for $\kappa > 0.03$. The sound level of the solid line is lower for $\kappa < 0.03$ and higher for $\kappa > 0.03$ than that of dotted lines, respectively. It is found that although the sound level of the dash line is lowest for $\kappa > 0.015$, the corresponding vibration level is always the highest in Figure 4(a); on the contrary, the sound levels of the dash and dotted lines are higher for $\kappa > 0.015$, the corresponding vibration levels always lower than that of the solid line. Besides, the vibration level of each case in Figure 4(a) is always higher than that of the case with the same thickness in Figure 3(a). It is because the resonant frequency ratios are not tuned to two. The smaller energy transfer to antisymmetrical modes results into the higher overall vibration.

Figure 5 shows the ratio of the antisymmetrical mode to symmetrical mode vibration levels for various resonant frequency ratios. It can be seen that if the resonant frequency ratio is closer to two, the antisymmetrical mode vibration level is higher. When the resonant frequency ratio is equal or close to two, the antisymmetrical mode vibration level is increasing against the excitation level for $\kappa < 0.02$, peaks around $\kappa = 0.02$, and decreasing for $\kappa > 0.02$. When the resonant frequency ratio is far from two, the antisymmetrical mode vibration level is monotonically increasing against the excitation level. The experiment data was obtained using the curved panel with a resonant frequency ratio of close to two. It is shown that that the experimental antisymmetrical mode vibration level is monotonically increasing against the excitation level; it only agrees well with the theoretical case in which the resonant ratio is 1.66. As the panel was not perfectly simply supported and symmetrical, that would result into a smaller energy transfer to the antisymmetrical mode. Thus the experiment data look likes the case of the resonant frequency ratio not tuned to two.

4. Conclusions

The nonlinear curved panels mounted a centre mass and the sound radiations have been studied. The results indicate that if the resonant frequency ratio is more far from two and the excitation and the structure are symmetrical, a higher excitation level is required to induce

the antisymmetrical mode vibration. In the frequency spectrums, it can be seen in some cases studied that the response frequency of the dominant mode, which is the first antisymmetrical mode, is much lower than the excitation frequency. This can be considered as "high-frequency excitation input-low-frequency response output." Besides, as the radiation efficiency of the antisymmetric mode is much lower than the others, the overall sound radiation is thus much smaller.

Appendix

Harmonic Balance Method

The harmonic balance method was employed for solving the Duffing equation, which represents the large amplitude free vibration of a beam in a previous study, and the result agreed well with the elliptic solution in [24]. Therefore, the method is selected here. As aforementioned, the single-mode approach is employed. Then, (2.3) can be reduced to the following form:

$$\ddot{q}_n + \varepsilon_1 q_n + \varepsilon_2 q_n^2 + \varepsilon_3 q_n^3 = 0, \tag{A.1}$$

where ε_1, ε_2, and ε_3 are the linear, quadratic, cubic nonlinear modal coefficients which depend on the mass, initial deflection, linear stiffness, nonlinear stiffnesses, and modal contribution factors; n is the mode number.

The solution of a nonlinear system is assumed to be of the form of a Fourier series:

$$q_n = C_0 + C_1 \cos(\omega_n t) + C_2 \cos(2\omega_n t) + \cdots, \tag{A.2}$$

$$C = C_0 + C_1 + C_2 + \cdots, \tag{A.3}$$

where $C_0, C_1, C_2 \ldots$ and so forth are the amplitudes of the harmonic components; C is the initial amplitude; ω_n is the resonant frequency.

For example, one constant and two harmonic terms are considered in (A.2). The Fourier expansion of the quadratic and cubic terms of the output $q(t)$ in (A.1) can be expressed, when retaining 2 harmonic components, as

$$\begin{aligned} q_n^2 &= \overline{C}_0 + \overline{C}_1 \cos(\omega_n t) + \overline{C}_2 \cos(2\omega_n t) \\ q_n^3 &= \overline{\overline{C}}_0 + \overline{\overline{C}}_1 \cos(\omega_n t) + \overline{\overline{C}}_2 \cos(2\omega_n t), \end{aligned} \tag{A.4}$$

where

$$\overline{C}_0 = \frac{\omega_n}{2\pi} \int_0^{2\pi/\omega_n} \left(C_0 + C_1 \cos(\omega_n t) + C_2 \cos(2\omega_n t)\right)^2 dt,$$

$$\overline{C}_1 = \frac{\omega_n}{2\pi} \int_0^{2\pi/\omega_n} \left(C_0 + C_1 \cos(\omega_n t) + C_2 \cos(2\omega_n t)\right)^2 \cos(\omega_n t) dt,$$

$$\overline{C}_2 = \frac{\omega_n}{2\pi}\int_0^{2\pi/\omega_n} (C_0 + C_1\cos(\omega_n t) + C_2\cos(2\omega_n t))^2\cos(2\omega_n t)dt,$$

$$\overline{\overline{C}}_0 = \frac{\omega_n}{2\pi}\int_0^{2\pi/\omega_n} (C_0 + C_1\cos(\omega_n t) + C_2\cos(2\omega_n t))^3 dt,$$

$$\overline{\overline{C}}_1 = \frac{\omega_n}{2\pi}\int_0^{2\pi/\omega_n} (C_0 + C_1\cos(\omega_n t) + C_2\cos(2\omega_n t))^3\cos(\omega_n t)dt,$$

$$\overline{\overline{C}}_2 = \frac{\omega_n}{2\pi}\int_0^{2\pi/\omega_n} (C_0 + C_1\cos(\omega_n t) + C_2\cos(2\omega_n t))^3\cos(2\omega_n t)dt. \tag{A.5}$$

Substituting (A.2) into (A.1) and equating coefficients associated with each harmonic component yields 3 equations as follows:

$$\begin{aligned} \varepsilon_1 C_0 + \varepsilon_2\overline{C}_0 + \varepsilon_3\overline{\overline{C}}_0 &= 0,\\ -\omega_n^2 C_1 + \varepsilon_1 C_1 + \varepsilon_2\overline{C}_1 + \varepsilon_3\overline{\overline{C}}_1 &= 0,\\ -\omega_n^2 C_2 + \varepsilon_1 C_2 + \varepsilon_2\overline{C}_2 + \varepsilon_3\overline{\overline{C}}_2 &= 0. \end{aligned} \tag{A.6}$$

There are four equations (A.3), (A.6) and four unknowns ω_n, C_0, C_1, C_2. Hence the resonant frequency ω_n, can be found.

Hamiltonian Approach

If the initial centre deflection, $q_o = 0$ in (2.3) (i.e., it is a flat panel), (A.1) can be rewritten in the following form:

$$\ddot{q}_n + \varepsilon_1 q_n + \varepsilon_3 q_n^3 = 0. \tag{A.7}$$

The Hamiltonian approach is now employed here for solving the Duffing equation in (A.1) to obtain the resonant frequency.

The Hamiltonian in (A.7) can be easily obtained, which reads

$$H = \frac{1}{2}\ddot{q}_n^2 + \frac{1}{2}\varepsilon_1 q_n^2 + \frac{1}{4}\varepsilon_3 q_n^4 = 0. \tag{A.8}$$

Integrating (A.8) with respect to t from 0 to $T/4$ yields

$$\overline{H}(q_n) = \int_0^{T/4}\left\{\frac{1}{2}\ddot{q}_n^2 + \frac{1}{2}\varepsilon_1 q_n^2 + \frac{1}{4}\varepsilon_3 q_n^4\right\}dt. \tag{A.9}$$

Consider that the solution can be expressed as $q_n = C\cos\omega_n t$ and substitute it to (A.9) as follows:

$$\overline{H}(q_n) = \frac{\pi}{8}C^2\omega_n + \frac{\pi}{8\omega_n}C^2\left[\varepsilon_1 + \frac{3}{8}\varepsilon_3 C^2\right]. \tag{A.10}$$

According to [3, 4], setting

$$\frac{\partial}{\partial C}\frac{\partial\overline{H}(u)}{\partial(1/\omega_n)} = 0. \tag{A.11}$$

By solving (A.11), the only unknown ω_n is given by

$$\omega_n = \sqrt{\varepsilon_1 + \frac{3}{4}\varepsilon_3 C^2}. \tag{A.12}$$

Acknowledgments

The work described in this paper was fully supported by a grant from the Research Grants Council of the Hong Kong, China [Project no. 9041496 (CityU 116209)]. The author would like to express his sincere gratitude and appreciation to Dr. WY Poon, Dr. CF Ng, and Ms. CK Hui for experimental hardware tuning and data acquisition.

References

[1] J.-H. He, "Some asymptotic methods for strongly nonlinear equations," *International Journal of Modern Physics B*, vol. 20, no. 10, pp. 1141–1199, 2006.
[2] J.-H. He, "Variational approach for nonlinear oscillators," *Chaos, Solitons & Fractals*, vol. 34, no. 5, pp. 1430–1439, 2007.
[3] J.-H. He, "Hamiltonian approach to nonlinear oscillators," *Physics Letters A*, vol. 374, no. 23, pp. 2312–2314, 2010.
[4] L. Xu and J. H. He, "Determination of limit cycle by Hamiltonian approach for strongly nonlinear oscillators," *International Journal of Nonlinear Sciences and Numerical Simulation*, vol. 11, no. 12, pp. 1097–1101, 2011.
[5] D. Younesian, H. Askari, Z. Saadatnia, and A. Yildirim, "Periodic solutions for the generalized nonlinear oscillators containing fraction order elastic force," *International Journal of Nonlinear Sciences and Numerical Simulation*, vol. 11, no. 12, pp. 1027–1032, 2011.
[6] A. Yildirim, Z. Saadatnia, and H. Askari, "Application of the Hamiltonian approach to nonlinear oscillators with rational and irrational elastic terms," *Mathematical and Computer Modelling*, vol. 54, no. 1-2, pp. 697–703, 2011.
[7] A. Yildirim, "Determination of periodic solutions for nonlinear oscillators with fractional powers by He's modified Lindstedt-Poincaré method," *Meccanica*, vol. 45, no. 1, pp. 1–6, 2010.
[8] C. K. Hui, Y. Y. Lee, and J. N. Reddy, "Approximate elliptical integral solution for the large amplitude free vibration of a rectangular single mode plate backed by a multi-acoustic mode cavity," *Thin-Walled Structures*, vol. 49, no. 9, pp. 1191–1194, 2011.
[9] Y. Y. Lee, "Structural-acoustic coupling effect on the nonlinear natural frequency of a rectangular box with one flexible plate," *Applied Acoustics*, vol. 63, no. 11, pp. 1157–1175, 2002.
[10] Y. Y. Lee, X. Guo, and E. W. M. Lee, "Effect of the large amplitude vibration of a finite flexible micro-perforated panel absorber on sound absorption," *International Journal of Nonlinear Sciences and Numerical Simulation*, vol. 8, no. 1, pp. 41–44, 2007.

[11] W. Y. Poon, C. F. Ng, and Y. Y. Lee, "Dynamic stability of a curved beam under sinusoidal loading," *Proceedings of the Institution of Mechanical Engineers G*, vol. 216, no. 4, pp. 209–217, 2002.
[12] X.-C. Cai and J.-F. Liu, "Application of the modified frequency formulation to a nonlinear oscillator," *Computers & Mathematics with Applications*, vol. 61, no. 8, pp. 2237–2240, 2011.
[13] G.-H. Chen, Z.-L. Tao, and J.-Z. Min, "Notes on a conservative nonlinear oscillator," *Computers & Mathematics with Applications*, vol. 61, no. 8, pp. 2120–2122, 2011.
[14] N. Herisanu and V. Marinca, "A modified variational iteration method for strongly nonlinear problems," *Nonlinear Science Letters A*, vol. 1, pp. 183–192, 2010.
[15] V. Marinca and N. Herisanu, "Optimal homotopy perturbation method for strongly nonlinear differential equations," *Nonlinear Science Letters A*, vol. 1, pp. 273–280, 2010.
[16] A. H. Nayfeh and D. T. Mook, *Nonlinear Oscillations*, Wiley-Interscience, New York, NY, USA, 1979.
[17] G. Schmidt and A. Tondl, *Nonlinear Vibrations*, Cambridge University Press, New York, NY, USA, 1986.
[18] Y. Y. Lee, R. K. L. Su, C. F. Ng, and C. K. Hui, "The effect of modal energy transfer on the sound radiation and vibration of a curved panel: theory and experiment," *Journal of Sound and Vibration*, vol. 324, no. 3-5, pp. 1003–1015, 2009.
[19] C. K. Hui, Y. Y. Lee, and C. F. Ng, "Use of internally resonant energy transfer from the symmetrical to anti-symmetrical modes of a curved beam isolator for enhancing the isolation performance and reducing the source mass translation vibration: theory and experiment," *Mechanical Systems and Signal Processing*, vol. 25, no. 4, pp. 1248–1259, 2011.
[20] Y. Y. Lee, W. Y. Poon, and C. F. Ng, "Anti-symmetric mode vibration of a curved beam subject to autoparametric excitation," *Journal of Sound and Vibration*, vol. 290, no. 1-2, pp. 48–64, 2006.
[21] Y. Shi, R. Y. Y. Lee, and C. Mei, "Finite element method for nonlinear free vibrations of composite plates," *AIAA Journal*, vol. 35, no. 1, pp. 159–166, 1997.
[22] F. Fahy, *Sound and Structural Vibration-Radiation, Transmission and Response*, Academic Press, 2000.
[23] Y. Y. Lee and C. F. Ng, "Sound insertion loss of stiffened enclosure plates using the finite element method and the classical approach," *Journal of Sound and Vibration*, vol. 217, no. 2, pp. 239–260, 1998.
[24] H. R. Srirangarajan, "Non-linear free vibrations of uniform beams," *Journal of Sound and Vibration*, vol. 175, no. 3, pp. 425–427, 1994.

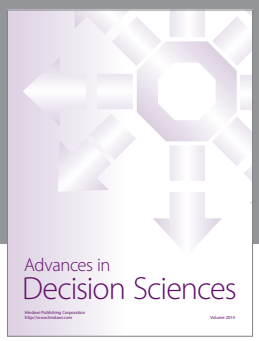

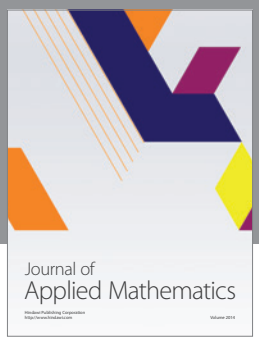

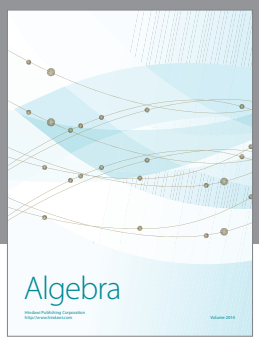

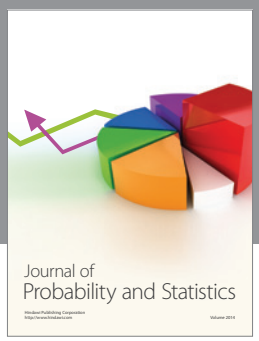

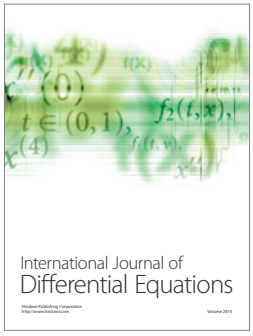

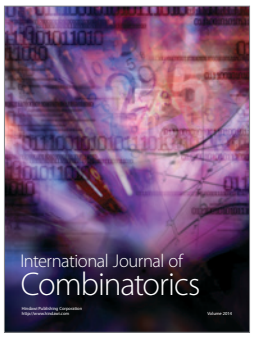

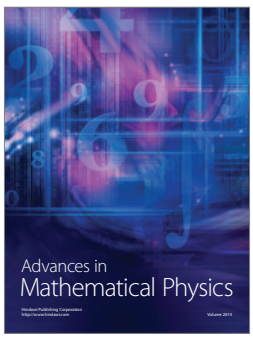

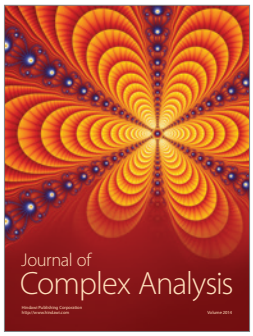

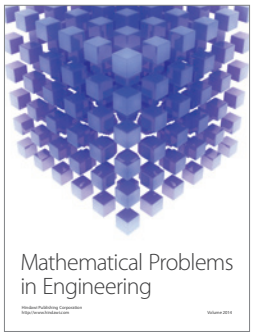

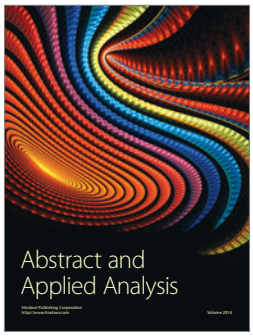

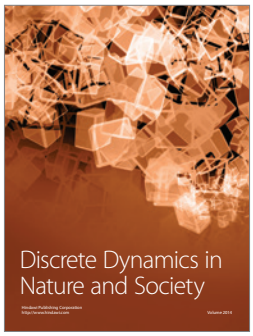

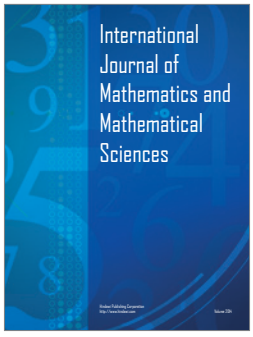

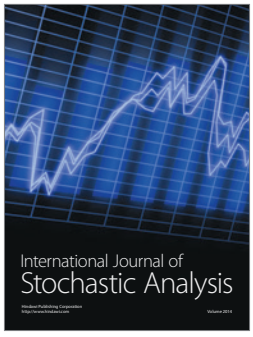

Hindawi
Submit your manuscripts at
http://www.hindawi.com